STATISTICAL ANALYSIS OF THE DISTRIBUTION OF TECTONIC FEATURES AND CRUSTAL THICKNESS IN THE NORTHERN HEMISPHERE OF MERCURY. Michelle M. Selvans[1], Thomas R. Watters[1], Peter B. James[2], and Sean C. Solomon[2,3], [1]Center for Earth and Planetary Studies, National Air and Space Museum, Smithsonian Institution, Washington, DC 20560, USA (selvansm@si.edu); [2]Lamont-Doherty Earth Observatory, Columbia University, Palisades, NY 10964, USA; [3]Dept. of Terrestrial Magnetism, Carnegie Institution of Washington, Washington, DC 20015, USA.

Introduction: Large thrust faults are found across the surface of Mercury [1, 2], primarily the result of contractional strain imparted by a decrease in radius as the planet cooled [3]. Here we examine prominent lobate scarps (single-sided faults) and high-relief ridges (double-sided), defined for this study as >50 km in length [4], similar in scale to the mechanical lithosphere thickness in which they developed [5]. Such features are not randomly distributed, as might be expected for faults resulting solely from radial contraction, implicating an additional source of heterogeneity in either stress or strength at the time of their formation [2, 4, 6].

We analyze geographical variations in modeled crustal thickness (CT) and mantle dynamic pressure (DP), as well as CT and DP values at the locations of tectonic features, in order to test the hypothesis that mantle flow may have spatially localized tectonic features at locations of relatively thick crust over sites of mantle downwelling [7]. Here we explore two CT models in the northern hemisphere of Mercury.

Background: Prominent scarps were first observed on Mercury in Mariner 10 images of about half the surface [1] and have been mapped across the entire surface [4] from orbital images taken by the Mercury Dual Imaging System on the MErcury Surface, Space ENvironment, GEochemistry, and Ranging (MESSENGER) spacecraft [8]. The total length of mapped prominent scarps in the northern hemisphere is ~1/3 of the global total [4], with cumulative lengths in the northern hemisphere of ~12,500 km for lobate scarps and ~1300 km for high-relief ridges.

Models of CT may be calculated for the northern hemisphere of Mercury from spherical harmonic representations of the gravity field derived from radio tracking and topography data from the Mercury Laser Altimeter [9, 10]. Because of MESSENGER's eccentric orbit and high northern periapsis, these data are at high resolution only in the northern hemisphere.

There are at least two methods by which we may construct CT maps from gravity and topography. We can determine the crust-mantle interface relief that minimizes the Bouguer gravity misfit [e.g., 9], or we can perform a dual inversion to solve for the distribution of deep mass anomalies along with CT [e.g., 10]. The first method requires fewer parameter assumptions, but the second removes the effect of deeper mass anomalies from the CT model.

In this analysis we use models calculated via both methods. We perform a Bouguer misfit minimization assuming a mean CT of 40 km and a crust-mantle density contrast of 250 kg/m^3 ("CT1"). The second CT model [10] ("CT2") was derived under the assumption of a 350 km depth for the deep mass anomalies. The dual inversion yields a map of dynamic mantle flow pressure in addition to the CT map. The DP map corresponds to either convective motion or viscous relaxation in the mantle (the latter in response to a perturbed interior interface or density anomalies) [11].

Methods: CT values are extracted at the center of each scarp segment. Linear segments of lobate scarps are ~23 km in length (559 segments), whereas high-relief ridge segments are ~38 km in length (35 segments). Cumulative scarp length is determined for bins of CT values defined by the mean and standard deviation of the CT areal coverage distribution.

We test CT and DP distributions for normalcy (χ^2 test with five degrees of freedom), and analyze distributions of scarp cumulative length with respect to these distributions, in order to determine whether scarps preferentially form within certain ranges of CT or DP.

Results: The simple CT model has a range of 4–76 km, mean X_{CT1} of 40.0 km, and standard deviation σ_{CT1} of 9.9 km. It has a χ_{CT1}^2 value of 0.86, which is consistent with a normal distribution for CT. The dual inversion model also has a normal distribution for CT (χ_{CT2}^2=0.82), with a range of 5–76 km, X_{CT2}=40.0 km, and σ_{CT2}=8.6 km. The DP associated with the dual inversion also follows a normal distribution (χ_{DP}^2=0.87), with a range of (-19.1–24.0)×10^6 N/m^2, X_{DP} of 0.0 N/m^2, and σ_{DP} of 5.9×10^6 N/m^2.

For the simple model (Fig. 1), scarps are found at crustal thicknesses of 22–73 km and a mean X_{S_CT1} of 44 km (σ_{S_CT1}=11 km). They are particularly concentrated (more than a factor of 1.5 greater than expected cumulative scarp length; 21% of scarps by length) in areas of thickest crust (>55 km), which cover 8% of the northern hemisphere. They are also particularly deficient (less than half the expected cumulative scarp length; 1% of scarps by length) in areas of thinnest crust (<25 km), which have 5% areal coverage.

For the dual inversion model, scarps are found at crustal thicknesses (Fig. 2) of 26–74 km, with X_{S_CT2}=42 km and σ_{S_CT2}=9 km. In this model, scarps are unusually concentrated (18% of scarps by length) in the thickest crust (>53 km), which cover 7% of the northern hemisphere. They are particularly deficient (1% of scarps by length) in areas of thinnest crust (<27 km), which have 4% areal coverage. Scarps are found at mantle DP values (Fig. 3) of (-14–22)×10^6 N/m^2, with X_{S_DP} of -1.5×10^6 N/m^2 and σ_{S_DP} of 5.6×10^6 N/m^2. Scarps are concentrated (61% by length) in areas of negative pressure (downward flow).

Discussion: Locations of prominent scarps in the northern hemisphere of Mercury are not randomly distributed with respect to CT, either for the simple model or for the model that includes mantle dynamics. In both cases, scarps are concentrated at locations with the thickest crust, by >2.5 times the expected cumulative length. Scarps are also concentrated in areas with negative mantle DP in the latter model.

These results are consistent with the hypothesis that flow in the mantle may have played a part in localizing faults in the lithosphere in areas of mantle downwelling and consequently thickened crust.

References: [1] Strom R.G. et al. (1975), *J. Geophys. Res. 80*, 2478-2507. [2] Watters T.R. et al. (2004), *Geophys. Res. Lett. 31*, L04701. [3] Solomon S.C. (1977), *Phys. Earth Planet. Inter. 15*, 135-145. [4] Watters T.R. et al. (2013), *Lunar Planet. Sci. 44*, 2213. [5] Watters T.R. and Nimmo F. (2010) in *Planetary Tectonics*, Cambridge Univ. Press, 15-80. [6] Watters T.R. et al. (2009), *Earth Planet. Sci. Lett. 285*, 283-296. [7] Selvans M.M. et al. (2013), *Lunar Planet. Sci. 44*, 2773, and references therein. [8] Solomon S.C. et al. (2001), *Planet. Space Sci. 49*, 1445-1465. [9] Smith D.E. (2012), *Science 336*, 214-217. [10] James P.B. (2013), Ph.D. thesis, Ch. 3, MIT. [11] James P.B. et al. (2014), *Lunar Planet. Sci. 45*, this mtg.

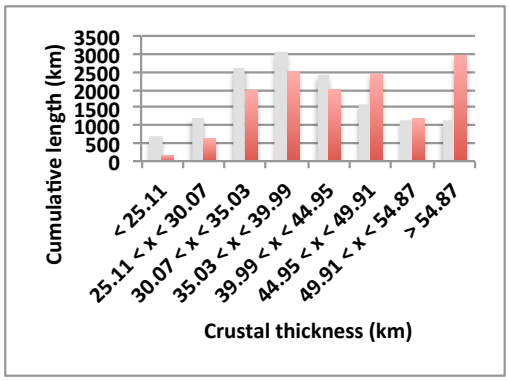

Fig. 1. Observed (red) scarp locations versus crustal thickness from CT1 and locations expected (gray) on the basis of the fractional areal coverage of each bin in the northern hemisphere. Bins are defined by the mean X and standard deviation σ of the crustal thickness distribution (the first two are < X-1.5σ and X-1.5σ < x < X-σ; others are defined by increments of 0.5σ).

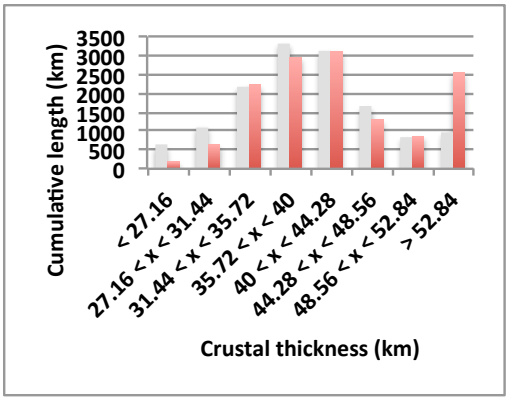

Fig. 2. Observed (red) and expected (gray) scarp locations vs. crustal thickness for CT2.

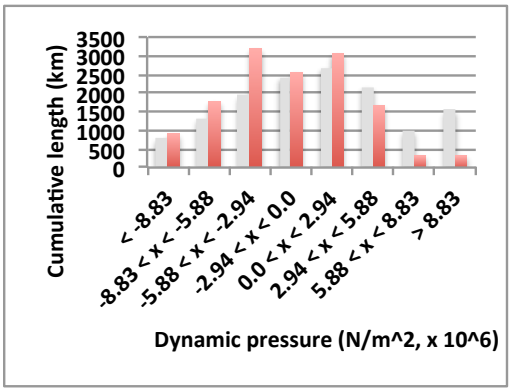

Fig. 3. Observed (red) and expected (gray) scarp locations vs. dynamic pressure from dual inversion.